LAWRENCE
LIVERMORE
NATIONAL
LABORATORY

LLNL-JRNL-605036

FIRST-PRINCIPLES STUDY OF THE PD-SI SYSTEM AND PD(001)/SIC(001) HETERO-STUCTURE

P. E. Turchi, V. I. Ivashchenko

November 28, 2012

Journal of Nuclear Materials

Disclaimer

First-principles study of the Pd-Si system and Pd(001)/SiC(001) hetero-structure

P.E.A. Turchi[a] and V.I. Ivashchenko[b]

[a]Lawrence Livermore National Laboratory (L-352), 7000 East Avenue, Livermore CA 94551, USA
[b]Institute of Problems of Materials Science, NAS of Ukraine, Krzhyzhanovsky str. 3, 03142 Kyiv, Ukraine

First-principles molecular dynamics simulations of the Pd(001)/3C-SiC(001) nano-layered structure were carried out at different temperatures ranging from 300 to 2100 K. Various PdSi (Pnma, $Fm\bar{3}m$, $P\bar{6}m2$, $Pm\bar{3}m$), Pd_2Si ($P\bar{6}2m$, $P6_3/mmc$, $P\bar{3}m1$, $P\bar{3}1m$) and Pd_3Si (Pnma, $P6_322$, $Pm\bar{3}m$, I4/mmm) structures under pressure were studied to identify the structure of the Pd/Si and Pd/C interfaces in the Pd/SiC systems at high temperatures. It was found that a large atomic mixing at the Pd/Si interface occurred at 1500-1800 K, whereas the Pd/C interface remained sharp even at the highest temperature of 2100 K. At the Pd/C interface, voids and a graphite-like clustering were detected. Palladium and silicon atoms interact at the Pd/Si interface to mostly form C22-Pd_2Si and $D0_{11}$-Pd_3Si fragments, in agreement with experiment.

I. INTRODUCTION

The properties of metal/SiC interfaces are of great importance in optoelectronics and high-temperature applications in metal/ceramic composites [1]. They are also relevant for the study of the metallurgical behavior of nuclear fuels in high-temperature gas-cooled reactors [2]. In that case the nuclear fuel kernel is coated with the so-called TRISO (tristructural-isotropic) coating consisting of four layers of three isotropic materials, C (porous buffer surrounding the fuel kernel), pyrolytic C, PyC, and SiC. In these coated fuels, the SiC layer sandwiched by PyC layers acts as a diffusion barrier to metallic fission products (*e.g.*, Pd, Cs, Sr), and also as a pressure vessel for the nuclear fuel particles and fission gases. In many of these applications, the reaction of a metal with SiC at the interface is of great importance for the control of the system functionality at high temperatures.

In this investigation, Pd has been chosen for studying the interface reaction in the Pd/SiC system. To our knowledge, this system has not yet been studied theoretically, despite the fact that the phase diagram of Pd-Si-C was widely investigated by experimental methods [3], and recently thermodynamically assessed [4]. The formation of periodic bands was observed in Pd/SiC diffusion couples with monocrystalline 6H-SiC [3]. The diffusion path is described as SiC/C+Pd_2Si/Pd_2Si – /C+Pd_2Si/Pd_2Si/Pd_3Si/Pd [3].

We have carried out molecular dynamics (MD) simulations of the Pd(001)/3C-SiC(001) couple at various temperatures. Several forms of PdSi, Pd_2Si, and Pd_3Si structures under pressure were also studied to identify the atomic configuration of Pd/Si and Pd/C interfaces in nano-layered Pd/SiC at high temperatures. It was found that a noticeable atomic mixing at the Pd/Si interface was occurring at 1500-1800 K, whereas the Pd/C interface remained sharp even at very high temperature. The palladium and silicon atoms interact at the Pd/Si interface to mostly form Pd_2Si and Pd_3Si fragments.

The paper is organized as follows. Sec. II is devoted to the computational methodology. In particular, the specific features of the calculations in the framework of a first-principles pseudo-potential (PP) method applied to the Pd-Si-C system are described in details. In Sec. III, the results of the calculations are presented and discussed. In particular, total energies of various Pd-Si structures under pressure, phonon spectra, and structural properties of Pd/SiC

nano-layered structures at various temperatures are analyzed. Finally, Sec. IV contains the main conclusions.

II. COMPUTATIONAL ASPECTS

Total energy calculations within the local-density approximation of density functional theory (DFT) were carried out using the Quantum-ESPRESSO first-principles code [5] for cubic, tetragonal, orthorhombic, and hexagonal unit cells of PdSi, Pd_2Si and Pd_3Si. The total energy (E_T) of the PdSi (space groups: Pnma, $Pm\bar{3}m$, $P\bar{6}m2$, $Pm\bar{3}m$), Pd_2Si (space groups: $P\bar{6}2m$, $P6_3/mmc$, $P\bar{3}m1$, $P\bar{3}1m$), and Pd_3Si (space groups: Pnma, $P6_322$, $Pm\bar{3}m$, I4/mmm) structures were calculated as functions of pressure to identify the possible Pd/SiC and Pd/CSi interfacial reactions that can take place in the Pd/SiC hetero-junction at high temperatures. The equilibrium geometry of each structure under consideration (except for the phases with two atoms per unit cell) was calculated with the Parinello-Rahman method [6] by relaxing both the ions and the unit cells while preserving the overall symmetry. Relaxations of the atomic coordinates and the unit cells were considered to be complete when the atomic forces were less than 1.0 mRy/bohr, the stresses were smaller than 0.05 GPa, and the total energy during the structural optimization iterative process was changing by less than 0.1 mRy. The structural and energetic characteristics of the relaxed phases at equilibrium were determined from the total energy (E_T) - cell volume (V), $E_T(V)$, dependences obtained by 6^{th}-order polynomial fitting to the DFT data points.

We employed also the first-principles code "Quantum ESPRESSO" [5] to perform molecular dynamics (MD) simulations of the Pd(001)/3C-SiC(001) couple at various temperatures. For this purpose, the initial tetragonal Pd (2×2×2)+3C-SiC (2×2×2) supercell consisting of 96 atoms was relaxed using the Parinello-Rahman variable-cell relaxation procedure [6]. Three-dimensional periodic boundary conditions were imposed. Under such conditions, the Pd/SiC couple represents a nano-layered structure with two interfaces: Pd/Si and Pd/C. MD simulations were then carried out in the constant number of particles – cell volume – temperature (NVT) ensemble at fixed temperature in the range 300-2100 K with an increment of 300 K. At each temperature step, the system was allowed to evolve during 0.3 ps. The high-temperature system, generated at 2100 K, was additionally equilibrated for 1 ps, and then relaxed to zero Kelvin using the Parinello-Rahman method [5,6]. We also performed MD simulations in the NVT ensemble for a 32-atom sample of fcc-based Pd at 2100 K for 1 ps.

In all the calculations, the ultra-soft pseudo-potentials were used [7]. The exchange-correlation interaction was considered in the generalized gradient approximation (GGA) [8]. To speed up convergence, each eigenvalue was convoluted with a Gaussian with a width σ = 0.02 Ry. Since we dealt with different structures, a similar setup was used for basis set, tail energies, and **k**-point mesh. The integration in the Brillouin zone was done with a set of special **k**-points determined according to the Monkhorst-Pack scheme [9] using the following meshes: (8 8 8) for the 2- 4-atomic unit cells; (4 4 8) and (6 6 6) for hexagonal structures with c/a~0.5, and c/a~1.0, respectively; (6 6 6) and (4 4 4) for the orthorhombic unit cells with 8 and 16 atoms, respectively. For the tetragonal unit cell of the Pd/SiC hetero-junction and the 32-atom fcc unit cell of Pd, only the Γ point was used. The cut-off energy (E_{cut}) for the plane-wave basis was set to 24 Ry. The reduced cut-off energy was used to minimize computer time (especially, in the case of large-scale MD simulations) without compromising accuracy. In the case of the different structures of the Pd-Si system, such selection was also found acceptable, since phase stability is estimated in a relative way. To further confirm this working assumption the effect of E_{cut} on the difference between the total energies of various structures of PdSi (ΔE_T) was examined. It was found that an increase of E_{cut} from 24 Ry to 40 Ry led to a scatter in ΔE_T that did not exceed 3 meV/atom, which was within the accuracy of first-principles calculations.

Finally, the Quantum-ESPRESSO first-principles code was used to calculate the phonon spectra of the orthorhombic MnP- and cubic CsCl-type PdSi structures in the framework of the density-functional perturbation theory (DFPT) [5,10].

III. RESULTS AND DISCUSSION

A. Pd-Si alloy system

In Table I we summarize the structural and energetic parameters of various structures of PdSi, Pd_2Si, and Pd_3Si at equilibrium. For each of these compounds, we have chosen the structural types that were experimentally observed for these and other compounds with the same formula unit. The most stable phases were found to be PdSi (Pnma), Pd_2Si ($P\bar{6}2m$) and Pd_3Si (Pnma), in agreement with experiment for the last two phases.

Table I. Space group, prototype structure, number of atoms in the unit cell (N), total energy (E_T) and formation energy (E^f) w.r.t fcc-Pd and diamond-Si (in eV/atom), equilibrium lattice parameters and bond lengths (in Å) of various calculated phases of PdSi, Pd_2Si, and Pd_3Si. The Pd-Pd, Pd-Si and Pd-C average bond lengths in the Pd/SiC system are 2.75, 2.43, and 2.10 Å, respectively.

Phase	Space group, No.	Type (N)	Struktur bericht Notation	E_T (eV/atom)	E^f (eV/atom)	Lattice parameters a,b,c (Å)	Bond length (Å)	
							Pd - Pd	Pd - Si
PdSi	Pnma 62	MnP (8) Orthorhombic	B31	-458.746	-0.540	5.631, 3.464, 6.163 (5.599, 3.381, 6.133)[a] (5.610, 3.385, 6.145)[b]	2.92 – –	2.5 2.55 2.6
	$Pm\bar{3}m$ 221	CsCl (2) Cubic	B2	-458.480	-0.274	3.066, 3.066, 3.066	3.07	2.66
	$P\bar{6}m2$ 187	WC (2) Hexagonal	B_h	-458.606	-0.400	3.603, 3.603, 2.745	2.75	2.49
	$Fm\bar{3}m$ 225	NaCl (2) Cubic	B1	-458.336	-0.130	5.034, 5.034, 5.034	3.56	2.52
Pd_2Si	$P\bar{6}2m$ 189	Fe_2P (9) Hexagonal	C22	-568.122	-0.685	6.524, 6.524, 3.582 (6.528,6.528, 3.437)[c] (6.497, 6.497, 3.433)[c]	2.87 2.88 2.99	2.43 2.49 2.55 2.69
	$P6_3/mmc$ 194	γ-W_2C (6) Hexagonal		-567.941	-0.504	4.216, 4.216, 5.742	2.83 2.87	2.44
	$P\bar{3}1m$ 162	ε-Fe_2N (9) Hexagonal		-567.965	-0.528	6.896, 6.896, 3.358	2.85	2.45
	$P\bar{3}m1$ 164	anti-CdI_2 (3) Hexagonal		-567.959	-0.423	3.892, 3.892, 3.557	2.87	2.42
Pd_3Si	Pnma 62	Fe_3C (16) Orthorhombic	$D0_{11}$	-622.653	-0.601	5.847, 7.744, 5.350 (5.735, 7.555, 5.260)[c]	2.84 2.87 2.96 2.97	2.38 2.48 2.65
	$P6_322$ 182	Fe_3C (4) Hexagonal		-622.399	-0.347	5.553, 5.553, 5.015	2.83 2.99	2.33
	$Pm\bar{3}m$ 221	Cu_3Au (4) Cubic	$L1_2$	-622.437	-0.385	3.886, 3.886, 3.886	2.748	2.748
	I4/mmm 139	Al_3Ti (8) Tetragonal	$D0_{22}$	-622.398	-0.346	4.595, 4.595, 5.606	4.288	2.692 2.789 3.248

[a]Ref. [11].
[b]Ref. [12].
[c]Ref. [13].

However in the case of the orthorhombic PdSi structure (B31, space group Pnma), this phase is supposed to be stable only at high temperatures between 1097 and 1245 K where congruent melting occurs, according to experimentally available data [14]. Although we find this phase to be the most stable among other PdSi structures considered here, this B31-PdSi may exhibit soft phonon modes which would explain why it is stabilized only at high temperatures. To verify this hypothesis, its phonon spectrum was calculated at equilibrium, and the final phonon density of states (PHDOS) is shown in Fig. 1. We note that the phonon spectrum does not contain any soft mode region around zero frequency, and therefore under these conditions one can expect that orthorhombic PdSi is quite stable at low temperatures. It follows that the stabilization of the B31-type PdSi structure at high temperatures observed experimentally is not related to its dynamical instability, and, most likely, to an entropy contribution relative to the nearby C22-Pd_2Si phase.

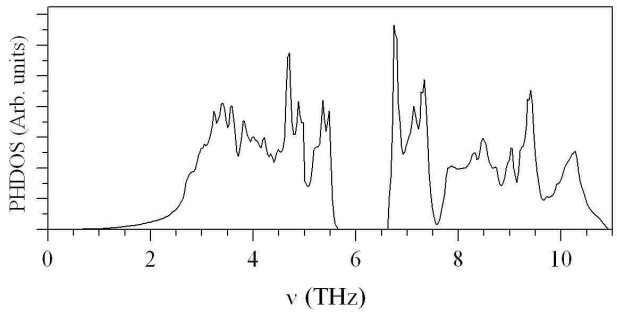

Figure 1. Phonon density of states (PHDOS) for the B31-type PdSi structure.

Let us return to the question about the influence of pressure on phase stability of different Pd-Si phases. In Fig. 2 we show the total energies of different PdSi, Pd_2Si, and Pd_3Si structures as functions of cell volumes (V). In the case of the PdSi structures, the results presented in Fig. 2 predict a first-order orthorhombic (MnP) to cubic (CsCl) phase transition under high pressure. We calculated the enthalpies (H) of both the MnP- and CsCl- type PdSi structures as functions of pressure (P). The results are shown in Fig. 3. According to these results, the transition pressure (P_0) is about 67 GPa, and the cell volume reduction is equal to 5.4%. For Pd_2Si and Pd_3Si, no pressure-induced phase transition was predicted.

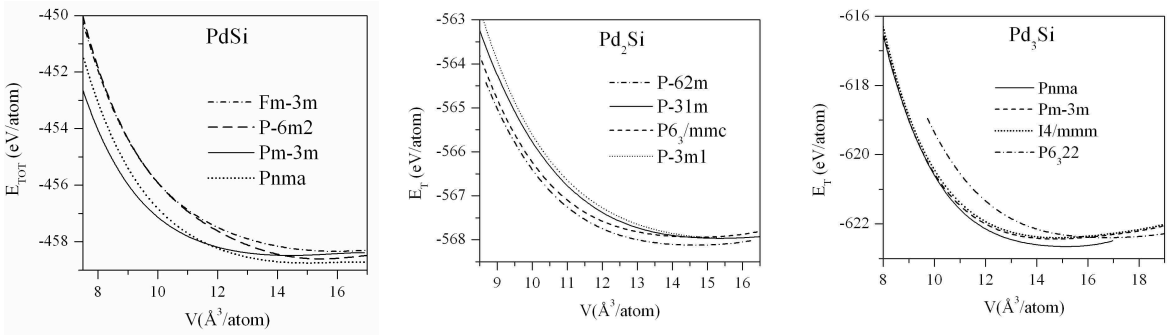

Figure 2. Total energy of various PdSi, Pd_2Si, and Pd_3Si phases as a function of cell volume.

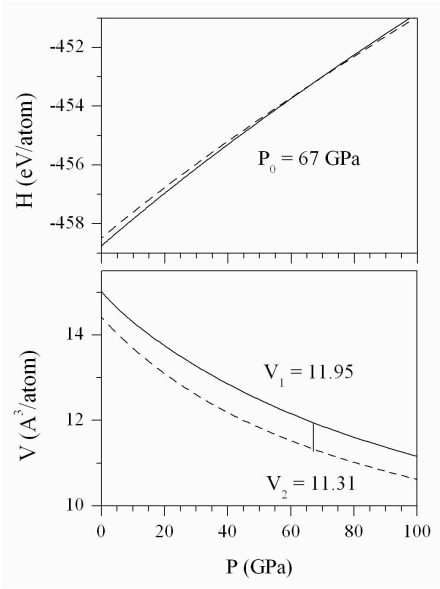

Figure 3. Enthalpy (H) and cell volume (V) of the Pnma (solid) and Pm $\bar{3}$m (dashed line) phases of PdSi as functions of pressure. P_0 is the transition pressure, and V_1, V_2 are the initial and final cell volumes (per atom) at P_0, respectively.

To search for a possible explanation for the pressure-induced stabilization of the CsCl-type (B2) PdSi phase we calculated its phonon spectrum at equilibrium and under pressure, P_0. The phonon dispersion curves along some symmetry directions of the Brillouin zone and the phonon density of states for the B2 PdSi structure at equilibrium and under pressure are presented in Figs. 4. At equilibrium, we find imaginary acoustic frequencies in the vicinity of the Γ point, which is incompatible with the dynamical stability of this phase. The analysis of the pressure dependence of the frequencies of the soft acoustic modes (not presented here) showed that the imaginary acoustic frequencies disappear at pressures above 39 GPa. This means that the pressure-induced cubic phase can exist only at high pressure (P>39 GPa), and the initial orthorhombic structure should be recovered after decompression.

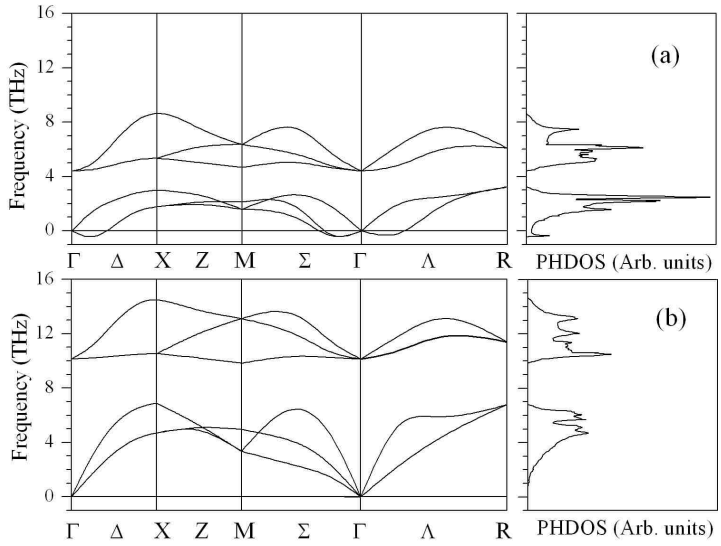

Figure 4. Phonon dispersion curves along some symmetry directions of the Brillouin zone (left panels) and phonon densities of states (PHDOS) (right panels) for the Pm $\bar{3}$m (B2, CsCl-type) PdSi structure under pressures P=0 GPa (a) and P=67 GPa (b).

To summarize this part of the study, the formation energies of all the structures studied are indicated in Table I, and displayed in Fig. 5. The end points that were considered are fcc-

based (A1) Pd (Total energy: -785.897162 eV/atom, a=3.978 Å, and B=162 GPa) and diamond-based (A4) Si, (Total energy: -130.515752 eV/atom, a=5.468 Å, and B=88 GPa), taken as zeros of energy in Fig. 5. We note that the maximum formation energy is associated with the C22 structure of Pd_2Si, which means that at the Pd/Si interface, the formation of this phase is likely to be preferred, in agreement with experimental findings [3]. The present results are compared in Fig. 5 with those from a recent thermodynamic assessment and phase diagram calculation based on the CALPHAD methodology [15]. Although in the Pd-Si phase diagram there are other complex phases that exist for Pd-rich alloys in addition to the three stoichiometries that have been considered in the present study (Pd_3Si, Pd_2Si, and PdSi), the agreement is quite reasonable except for PdSi, which is reported to be stable at temperature, between 1097 and 1245 K [14]. It is worth noting that since the data from CALPHAD are usually assessed well above room temperature, the comparison with *ab initio* data, obtained at 0 K, are therefore only indicative. However in both approaches (*ab initio* results and CALPHAD assessment), the heat of formation of the Pd_2Si compound is the most negative.

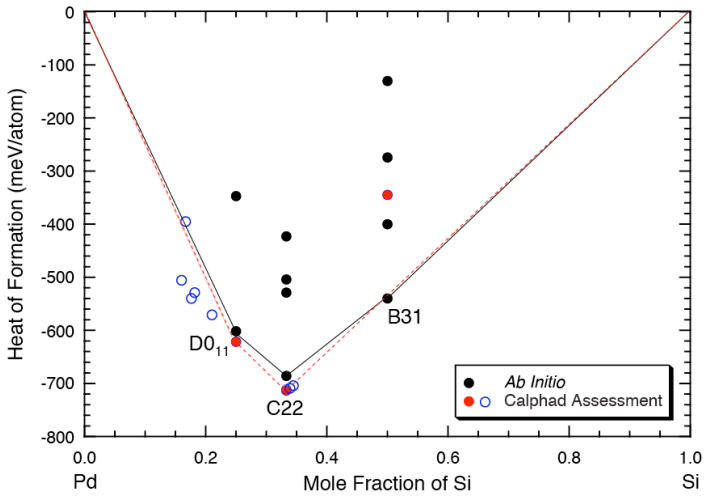

Figure 5. *Ab initio* heats of formation (black circles) of the various compounds of the Pd-Si system listed in Table II. For comparison, results from a recent thermodynamic assessment based on the CALPHAD methodology [15] are also reported. Fcc (A1) Pd and diamond (A4) Si are taken as zeroes of energy. The (blue) red circles indicate those data from Ref. 15 (not) considered in this work.

B. Pd/SiC heterostructures

Step-by-step MD simulations were carried out for the Pd/SiC couple at various temperatures. Beginning at 300 K and for each temperature step of 300 K up to 2100 K the atomic configuration and the total energy of the nano-layered structure were analyzed. Useful information on atomic mixture at the Pd/Si and Pd/C interfaces can be extracted from the analysis of the density profile in the z-direction, *i.e.*, along the layered structure. This function is shown in Fig. 6. The total energy at each temperature step is presented in Fig. 7. Comparing the results shown in Figs. 6 and 7 we conclude that the sharp Pd/Si interface begins to diffuse between 1200 and 1500 K. At 1500 K the four-peak structure of the Pd density profile transforms to a three-peak structure. In addition, a strong mixture of the Pd and Si atoms at the Pd/Si interface takes place. On the contrary, the Pd/C interface remains sharp even at the highest temperature of 2100 K. Above 1500 K, the atomic mixture at the Pd/Si interface continues, although it is accompanied with a small change in E_T (cf. Fig. 7). Hence, we predict that, at approximately 1500 K, the Pd_2Si and Pd_3Si phases start to form. Once these phases form, a further increase in temperature would cause a large increase in total energy.

Let us now examine the atomic configuration of the Pd/SiC system heated at higher temperatures. Here we focus on the study of this system equilibrated at 2100 K with subsequent relaxation. The atomic configuration of the resultant sample is shown in Fig. 8. One can see that the Pd/Si interface in the high-temperature structure is wider by ~ 3 Å as compared to those that have been observed in the low-temperature structures. On the contrary, the Pd/C interface remains sharp, *i.e.*, no mixing among C and Pd species is observed. Moreover, a void and a carbon cluster form at this interface. The latter is confirmed by the shape of the pair-correlation function (PCF) of the SiC slab in the Pd/SiC nano-layered system. These functions for the low-temperature and high-temperature structures are presented in Fig. 9. The appearance of the nearest neighbor C-C correlations at 1.44 Å clearly indicates the formation of a graphite-like clustering. We note that an increase in temperature leads to a shift at higher distance of all the peaks in the PCF of the SiC slab due to anharmonic effect. Except for the C layers at the Pd/C interface, the 3C-SiC structure of the SiC slab is preserved even at 2100 K, cf. Fig. 9.

To identify in more details the structures of the Pd slab, the Pd/Si and Pd/C interfaces in the high-temperature Pd/SiC nano-layered system we calculated the partial PCFs and bond-angle distributions g(Θ) related to the Pd-Pd, Pd-Si and Pd-C correlations. These functions are shown in Figs. 9 and 10 in comparison with those for the A1-Pd, B31-PdSi, C22-Pd_2Si and $D0_{11}$-Pd_3Si phases. The position of the PCF peaks related to the second- and third-nearest neighbor correlations indicates the amorphous structure of the Pd slab. One can see from Fig. 9 that bulk fcc-based Pd heated to 2100 K shows the features of the amorphous structure. Upon quenching, the crystalline structure of this sample was recovered (not shown here). And therefore, what remains of the amorphous structure of the Pd slab in the Pd/SiC couple upon quenching is due to the distorted interfaces.

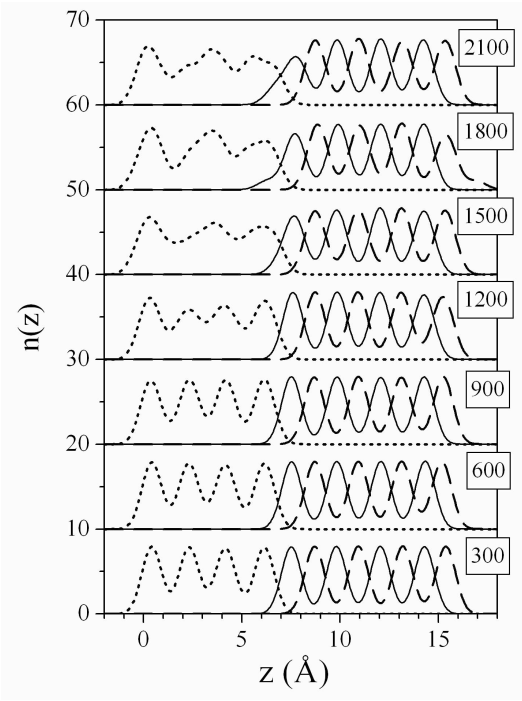

Figure 6. Density profile in the z-direction of the Pd-SiC layered system. The distribution of the Pd, Si and C atoms are shown as dotted, solid and dashed lines, respectively.

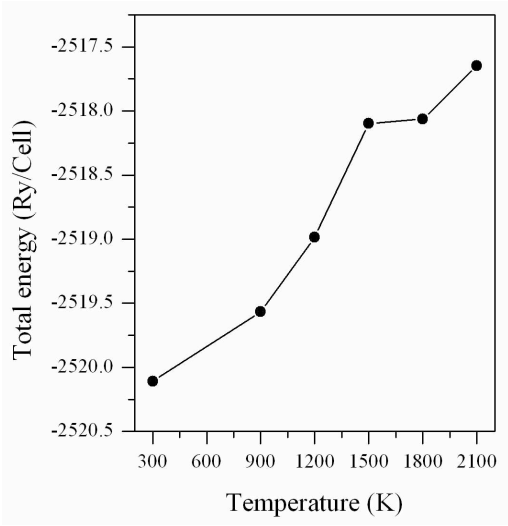

Figure 7. Total energy of the Pd-SiC layered structure as a function of temperature. The total energies correspond to the structures equilibrated for 0.3 ps (*i.e.*, 300 time steps), when a change in the total energy during several time steps did not exceed 0.0005 Ry.

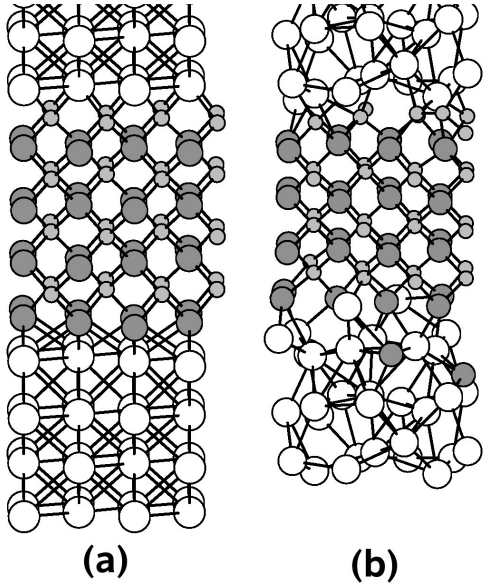

Figure 8. Atomic configuration of the Pd/SiC system equilibrated at 300 K (a) and 2100 K (b).

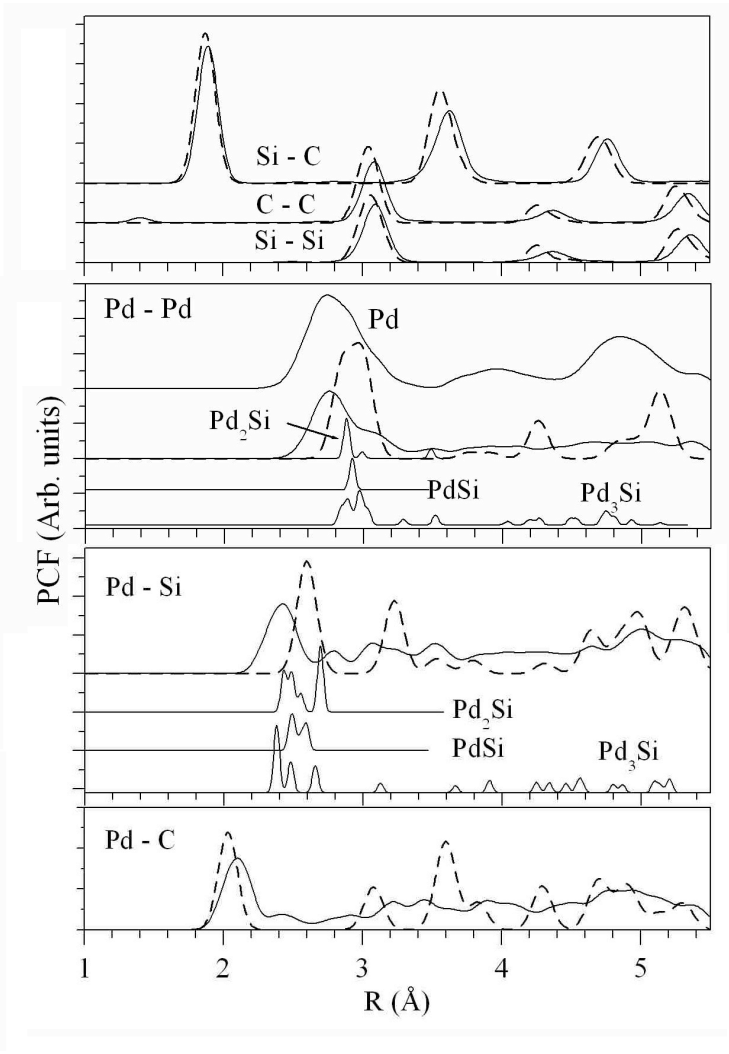

Figure 9. Pair correlation functions (PCF) of the Pd/SiC hetero-structures equilibrated at 300K (dashed line) and 2100 K (solid line) in comparison with those of the Pd-Si phases.

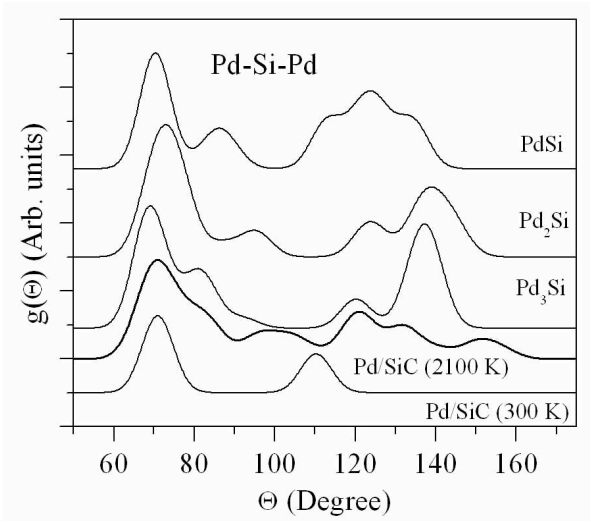

Figure 10. Si-Pd-Si bond angle distributions, g(θ), of Pd/SiC systems equilibrated at 300K and 2100 K in comparison with those of the Pd-Si phases.

An analysis of the results presented in Fig. 9 shows that the distance of the nearest neighbor Pd-C pair correlation increases with temperature, whereas the distance of the nearest neighbor Pd-Si pair correlations decreases. This means that, in the Pd/SiC nano-layered system, at high temperatures, a delamination of the Pd and C layers takes place at the Pd/C interface, and an enhancement of the Pd-Si interactions occurs at the Pd/Si interface. As a result, the voids appear at the Pd/C interface, and the new Pd-Si phases form at the Pd/Si interface. In order to identify these phases we calculated several possible structures belonging to the PdSi, Pd_2Si, and Pd_3Si formula units, assuming that some of them could form at very high temperatures at the Pd/Si interface. The structural parameters of these phases are summarized in Table I. An analysis of the data presented in Table I, as well as a comparative examination of the PCFs and $g(\Theta)$ of the ground state PdSi, Pd_2Si and Pd_3Si (cf. Fig. 9 and 10) enabled us to establish the main structures that are formed at the Pd/Si interface. These are fragments of the hexagonal (space group $P\bar{6}2m$) C22-Pd_2Si and, to a less extent, orthorhombic (space group Pnma) $D0_{11}$-Pd_3Si structures, in agreement with experimental observations [3].

IV. CONCLUSION

We carried out molecular dynamics simulations for the nano-layered Pd(001)/3C-SiC(001) structure from room temperature top 2100 K. Various PdSi (Pnma, $Fm\bar{3}m$, $P\bar{6}m2$, $Pm\bar{3}m$), Pd_2Si ($P\bar{6}2m$, $P6_3/mmc$, $P\bar{3}m1$, $P\bar{3}1m$) and Pd_3Si (Pnma, $P6_322$, $Pm\bar{3}m$, I4/mmm) structures under pressure were studied to identify the structure of the Pd/Si and Pd/Ci interfaces in the Pd/SiC systems at elevated temperatures. The results predict an orthorhombic-to-cubic first-order phase transition in PdSi at a pressure of 67 GPa. This transition is reversible, since the pressure-induced CsCl-type (B2) PdSi phase has soft acoustic modes below 39 GPa. For Pd_2Si and Pd_3Si, the hexagonal and orthorhombic structures, respectively, are the ground-state structures, and remain stable under pressure. It was found that, in the Pd/SiC couple, a large atomic mixing at the Pd/Si interface occurred at 1500-1800 K, whereas the Pd/C interface stays sharp even at very high temperature. At the Pd/C interface, voids and a graphite-like clustering are detected. The silicon atoms interact with the palladium atoms at the Pd/Si interface forming mostly C22-Pd_2Si and $D0_{11}$-Pd_3Si fragments, in agreement with experiment.

ACKNOWLEDGEMENT

The work of P.T. was performed under the auspices of the U. S. Department of Energy by the Lawrence Livermore National Laboratory under contract No. DE-AC52-07NA27344. The work of V.I. was supported by the STCU contract No. 5539.

REFERENCES

[1] R. Leucht and H. J. Dedek, Mater. Sci. Eng. **A188**, 201 (1994).
[2] T. Ogawa and K. Ikawa, High. Temp. Sci. **22**, 179 (1986).
[3] K. Bhanumurthy and R. Schmid-Fetzer, Z. Metalkd. **87**, 61 (1996).
[4] Z. Du, C. Guo, X. Yang, and T. Liu, Intermetallics **14**, 560-569 (2006).
[5] S. Baroni, A. Dal Corso, S. de Gironcoli, P. Giannozzi, C. Cavazzoni, G. Ballabio, S. Scandolo, G. Chiarotti, P. Focher, A. Pasquarello, K. Laasonen, A. Trave, R. Car, N. Marzari, and A. Kokalj, http://www.pwscf.org/.
[6] M. Parrinello and A. Rahman, Phys. Rev. Lett. **45**, 1196 (1980).
[7] D. Vanderbilt, Phys. Rev. **B 41**, 7892 (1990).
[8] J. P. Perdew, K. Burke, and M. Ernzerhof, Phys. Rev. Lett. **77,** 3865 (1996**)**.
[9] H. J. Monkhorst and J. D. Pack, Phys. Rev. **B13,** 5188 (1976).

[10] S. Baroni, S. de Gironcoli, A. Dal Corso, and P. Giannozzi, Rev. Mod. Phys. **73**, 515 (2001).
[11] H. Pfisterer and K. Schubert, Z. Metallkd. **41**, 358 (1950).
[12] K. Goeransson, I. Engstroem, and B. Nolaeng, J. Alloys and Compounds, **219**, 107 (1995).
[13] B. Aronsson and A. Nylund, Acta Chemica Scandinavica, **14,** 1011 (1960).
[14] H.V. Baxi and T. B. Massalski, J. Phase Equilibria **12**, 349 (1991); and references therein.
[15] Zhenmin Du, Cuiping Guo, Xiaojian, and Ting Liu, Intermetallics **14**, 560 (2006).